

## DIS and related processes in QCD

In this chapter we complete our treatment of inclusive structure functions for DIS in QCD. Our analysis so far started with the parton model, and we generalized it to a factorization property, for which we found a complete proof in a non-gauge theory in Sec. 8.9. We then formulated factorization in QCD (without a proof), using gauge-invariant definitions of parton densities from Sec. 7.6. This enabled us to make low-order calculations of the perturbative hard-scattering coefficients in Ch. 9

The methods of Ch. 10 allow us to complete the work for QCD. Compared with a non-gauge theory, there is no change in the form of factorization, i.e., (8.81) and (8.83). The DGLAP evolution equations, associated with the renormalization of parton densities, are also unchanged in structure.

One change in QCD is that the operators defining the parton densities acquire Wilson lines; we also need to justify the form of the gluon density. For the proof, the enhancements relative to Sec. 8.9 are caused by the extra gluons joining the hard and collinear subgraphs in leading regions. We need generalization beyond the related work in Ch. 10 because the gauge group of QCD is non-abelian. The subtractions in the hard scattering are more complicated than those with the ladder structures appropriate to a non-gauge theory. Finally, in generalizing DIS to an off-shell Green function instead of an on-shell matrix element, we need extra parton-density-like quantities involving gauge-variant operators.

### 11.1 General principles

The steps to obtain factorization are:

1. List the regions as specified by PSSs in the massless limit of the theory (Ch. 5). These are labeled by subgraph decompositions like Fig. 11.1(b).
2. Find those regions that are leading, as in Sec. 5.8.
3. To leading power, write the amplitude as a sum over contributions for each region of each graph:  $\sum_{R,\Gamma} C_R \Gamma$  (Sec. 10.1). Subtractions in  $C_R \Gamma$  compensate double counting between regions.
4. Diagrams like Fig. 11.1(b) now acquire extra meanings:
  - The subgraph decomposition can symbolize a particular  $C_R \Gamma$ .
  - The diagram can imply a sum over  $R$  and  $\Gamma$ , and hence a sum over the Feynman graphs for each subgraph. Thus, it almost denotes the factorization property.

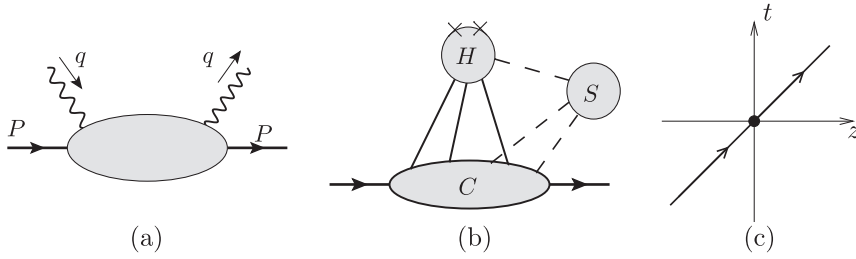


Fig. 11.1. (a) Uncut amplitude  $T^{\mu\nu}$  for DIS. (b) General reduced graph for  $T^{\mu\nu}$ . (c) Space-time structure of its massless PSSs when  $x \neq 1$ .

5. The factors in  $C_R\Gamma$  are defined from a power-series expansion in parameters/variables that the region  $R$  labels as small. (But renormalization, etc. is applied as needed to prevent divergences from momenta in larger regions.)
6. Finally we apply Ward identities. This, for example, extracts extra collinear gluons attaching to the hard subgraph and converts them to a Wilson-line form, as in Sec. 10.8. Methods from that section ensure that subtractions and renormalization are compatible with the Ward identities.

Note that Ward identities are not compatible with a naive region analysis, i.e., one where momentum space is partitioned into categories of hard, soft, etc., with boundaries between the regions, and where each region subgraph is defined to have its momenta restricted to the subgraph’s category. But a proof of a Ward identity involves shifts of loop-momentum variables. Particularly when momenta are close to boundaries of regions, shifts of loop momenta can take them across boundaries; thus the shifted momenta can be of different categories. This was a primary motivation to define the region contributions  $C_R\Gamma$  with unrestricted integrals over loop momenta.

### 11.2 Regions and PSSs, with uncut hadronic amplitude

As we saw in Sec. 5.3.3, the analysis of regions for DIS is simpler for the *uncut* amplitude, Fig. 11.1(a),

$$T^{\mu\nu}(q, P) = \frac{1}{4\pi} \int d^4z e^{iq \cdot z} \langle P, S | T j^\mu(z/2) j^\nu(-z/2) | P, S \rangle, \quad (11.1)$$

from which the ordinary structure tensor is obtained as a discontinuity across the physical-region cut:  $W^{\mu\nu}(q, P) = T^{\mu\nu}(v + i0) - T^{\mu\nu}(v - i0)$ .

As usual, the relevant regions are determined by PSSs corresponding to physical scattering of massless particles, with a general reduced graph typified in Fig. 11.1(b). It has collinear and hard subgraphs with a possible connecting soft subgraph. The space-time structure is shown in Fig. 11.1(c): there is a short-distance scattering at the vertex for the virtual photon, while the collinear subgraph and the target hadron correspond to the diagonal (light-like) line.

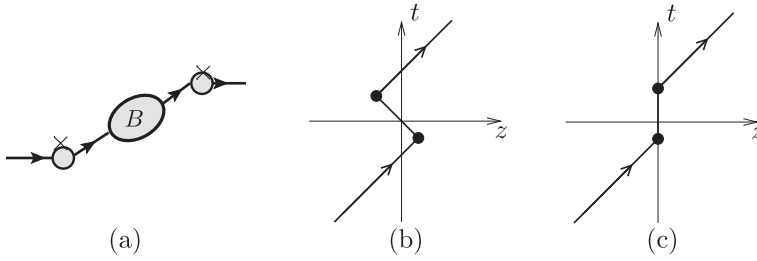


Fig. 11.2. (a) Reduced graph for  $T^{\mu\nu}$  at  $x \simeq 1$ . Not indicated are extra collinear lines and a possible soft subgraph. (b) Space-time structure of its massless PSSs when  $x = 1$ . (c) Same with massive intermediate state.

### 11.2.1 Local averaging

This picture fails when  $x$  is close to unity, i.e., where  $(P + q)^2 \simeq Q^2(1 - x)/x$  gets small. In that case we can have a reduced graph like Fig. 11.2(a), where there is an intermediate state whose mass is small compared with  $Q$ . For simplicity, a possible soft subgraph has been omitted. The corresponding PSS has a massless system going in the minus direction, Fig. 11.2(b). Possible intermediate states include a single proton (giving elastic scattering) and low-mass resonances. If we work in perturbation theory with an elementary quark target, instead of a hadron target, we have emission of soft and of final-state-collinear quanta, as in the NLO calculations in Ch. 9.

A full analysis of this region needs more sophisticated methods than we use here. Instead, we obtain the standard factorization formalism by the averaging method used in Secs. 4.1.1 and 4.4 for the total hadronic cross section for  $e^+e^-$  annihilation. In DIS we use an average in  $x$ :

$$T^{\mu\nu}[f] = \int dx T^{\mu\nu}(q, P) f(x), \tag{11.2}$$

with a smooth function  $f(x)$ . In the uncut amplitude, the troublesome final-state singularities all lie on one side of the real  $x$  axis, e.g.,

$$\frac{i}{Q^2(1-x)/x - m^2 + i0} = \frac{ix/Q^2}{1-x - m^2/Q^2 + i0}. \tag{11.3}$$

Thus we can deform<sup>1</sup> the integration contour away from the singularities. Then the relevant propagators are off-shell by order  $Q^2$ , and the leading regions return to the form of Fig. 11.1(b), for all  $x$ , and our standard derivations will now apply. Then the difference between  $T^{\mu\nu}[f]$  and its complex conjugate gives a valid prediction for the locally averaged structure functions.

The averaging method also solves another conceptual problem. This is that in a theory with confined quarks, the evolution of the final state might be more like that of an elastic spring than of a fragile string, to use the terminology of Sec. 4.3.1. In that case a final state

<sup>1</sup> Strictly, a test function  $f$  need not be an analytic function, which makes questionable a contour deformation. But a basis set of analytic functions, e.g., Gaussians, suffices for our argument.

of a high-energy struck quark and a target remnant would evolve not to a pair of connected jets, but to a spectrum of bound states or of narrow resonances.

Standard factorization methods do not describe the bound-state structure. Thus, the true predictions of factorization are only for locally averaged structure functions. This has been verified by Einhorn (1976) in a model with elastic spring confinement: QCD in two space-time dimensions in the limit of a large number of colors. Only if the structure functions are already smooth does factorization apply point-by-point.

We already saw the need for local averaging in our NLO calculations in Ch. 9. There we found a cancellation between real and virtual emission of gluons that are soft or are final-state collinear. The cancellation was embodied in the plus distribution in the coefficient functions, e.g., (9.20). At large  $x$ , the necessary average must be done by the local averaging of the hadronic structure functions. But at smaller  $x$ , it suffices to use the integral over parton momentum in the factorization formula (8.81), provided that the parton densities are sufficiently smooth.

### 11.2.2 Parton-hadron duality

At large  $x$  and moderate  $Q^2$ , there are many noticeable resonances in DIS structure functions. That partonic methods can nevertheless be applied, but only to locally averaged structure functions, is an instance of the concept called parton-hadron duality. It was first found before the advent of QCD and factorization theorems in an analysis of data by Bloom and Gilman (1971). Duality carries the implication that the partonic structure and the resonance structure are parts of the same overall mechanism, rather than two distinct mechanisms to be added to each other.

For a recent review, see Melnitchouk, Ent, and Keppel (2005). One of their comparisons with recent data is shown in Fig. 11.3. As  $Q^2$  is increased, the resonances move to the right in  $x$ , a necessary kinematic property. This is not compatible with the generally smooth scaling violations given by DGLAP evolution. Naturally the spacing of the resonances in  $x$  decreases as  $Q^2$  increases. But there is little or no decrease in the height of the resonances, as a fraction of the structure function.

Much of the phenomenological application of duality is at low  $Q^2$ , where the region of noticeable resonances extends a long way down in  $x$ . But even at large  $Q^2$ , resonances remain, close to  $x = 1$ . According to duality, the smooth curves for  $F_2$  from factorization should cross the resonance oscillations approximately midway between their peaks and troughs. However, with the MRST fit shown in Fig. 11.3, this appears *not* to be the case, at least for the larger values of  $Q^2$ . The reasons are unclear; the CTEQ and MRST curves disagree.

### 11.2.3 Leading and super-leading terms

We now restrict our attention to those regions that contribute at the leading power,  $Q^0$ , or larger, determined by the methods of Sec. 5.8. The basic rule is that increasing the number of lines connecting the hard and collinear subgraphs gives a suppression, as does

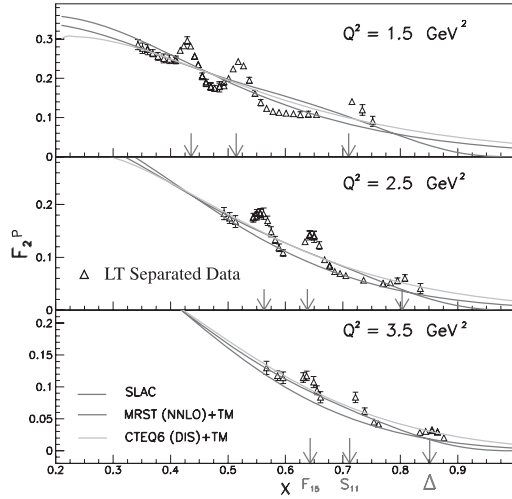


Fig. 11.3. Proton structure function  $F_2^p$  measured at Jefferson Lab Hall C. Two of the smooth curves are the results of QCD fits to other data by MRST (Martin *et al.*, 1998) and CTEQ (Lai *et al.*, 2000), with target mass corrections included by the method of Barbieri *et al.* (1976). The SLAC curve is a fit to DIS data (Whitlow *et al.*, 1992). The arrows indicate the positions of prominent resonances. Reprinted from Melnitchouk, Ent, and Keppel (2005), with permission from Elsevier.

the presence of a soft subgraph. But, just as with the Sudakov form factor in Ch. 10, there is an exception for collinear gluons of polarization in the plus direction; dealing with these is the main difficulty in our proof. The proof will be organized differently than in Ch. 10, in order to overcome the complications of working in a non-abelian gauge theory.

Of the lines entering the hard scattering  $H$  from the collinear subgraph  $C$ , let  $N$  be gluons, for which we write the polarization sum as

$$H \cdot C = H_{\mu_1 \dots \mu_N} \prod_{j=1}^N g^{\mu_j \nu_j} C_{\nu_1 \dots \nu_N}. \tag{11.4}$$

Let  $k_j$  be the momentum of gluon  $j$  flowing into  $H$ . The largest term in its polarization sum has  $\mu_j = -, \nu_j = +$ , and we manipulate it into a form suitable for the use of Ward identities. Accordingly, we make a Grammer-Yennie decomposition

$$g^{\mu_j \nu_j} = K^{\mu_j \nu_j} + G^{\mu_j \nu_j}, \tag{11.5}$$

where

$$K^{\mu_j \nu_j} = \frac{k_j^{\mu_j} w_2^{\nu_j}}{k_j \cdot w_2 - i0}, \quad \text{and} \quad G^{\mu_j \nu_j} = g^{\mu_j \nu_j} - \frac{k_j^{\mu_j} w_2^{\nu_j}}{k_j \cdot w_2 - i0}, \tag{11.6}$$

and the vector  $w_2$  projects onto plus components of momentum:  $w_2 = (0, 1, \mathbf{0}_T)$ . Then from (11.4), we get a sum of terms which we label by saying that each of the gluons is a  $K$  gluon or a  $G$  gluon according to which term in (11.5) is used.

The denominators  $k_j \cdot w_2$  introduce singularities at  $k_j^+ = 0$ , that have no corresponding actual singularities in  $H$ . In the final result, we will find a cancellation of these artificial singularities. We choose to equip the singularities with an  $i0$  prescription appropriate for a final-state pole; it must be the same in all terms for our Ward identities to work.

(Notice a contrast with the situation for the Sudakov form factor, for which hard-scattering subgraphs often had singularities for soft and for opposite-side collinear configurations. These were canceled by subtractions for smaller regions. To ensure contour-deformation arguments for the Glauber region worked, we found that the  $i0$  prescription for the denominators  $k_j \cdot w_2$  had to correspond to that of the subtracted singularities in the hard-scattering subgraph.)

The normal suppression for extra collinear lines entering the hard scattering applies to the  $G$  gluons but not to the  $K$  gluons (Sec. 5.8). For a collinear gluon with radial coordinate  $\lambda$ , the  $K$  term has a power  $Q/\lambda$  relative to the  $G$  term.

Complications now arise when all the lines connecting the hard and collinear subgraphs are  $K$  gluons, because they give super-leading contributions from individual graphs, with a power  $Q^2/\lambda^2$  relative to the final result. This also permits there to be a soft subgraph at leading power. There is in fact a cancellation (Labastida and Sterman, 1985) of super-leading terms in the sum over graphs. Although in a model with an abelian gluon field the cancellation of  $K$  gluons is exact, in QCD there are left-over leading-power terms (Collins and Rogers, 2008), and these are needed for factorization.

After the Grammer-Yennie decomposition, we can define two classes of contribution. The first has a pair of ordinary leading-power partons accompanied by any number of  $K$  gluons. In these situations, the lines joining the collinear and hard subgraphs are:

1. two  $G$  gluons plus any number of  $K$  gluons;
2. or: a quark and an antiquark line plus any number of  $K$  gluons;
3. or: a ghost and an antighost line plus any number of  $K$  gluons. One of the simplest graphs with such a region is shown in Fig. 11.4.

In all the above cases, there is no soft subgraph, and we have a leading-power ( $Q^0$ ) contribution. Adding extra  $G$  gluons, quarks, ghosts, or a soft subgraph gives a power-suppression.

The case with collinear ghost lines does not correspond to any term in the factorization theorem. Instead we will find it combines with part of the next class of contributions to give a result that vanishes in physical quantities.

A second class of terms covers the remaining possibilities for leading and super-leading powers. In these, all the collinear lines entering the hard scattering are gluons:

1. If all of the gluons are  $K$  gluons and there is no soft subgraph, we have a super-leading contribution of order  $Q^2$ .
2. If all but one of the gluons is a  $K$  gluon, we have a super-leading contribution of order  $Q^1$ .
3. A soft subgraph contributes a suppression, but may leave the contribution leading.

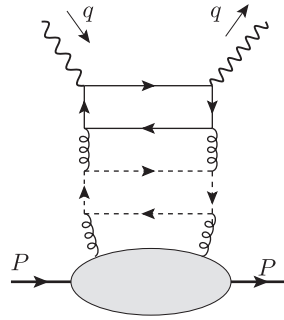


Fig. 11.4. Graph for DIS with Faddeev-Popov ghost loop.

All other cases give a power-suppression. From Sec. 5.8, the only case that a soft subgraph allows a leading-power contribution is where all the collinear attachments to  $H$  are  $K$  gluons, the external lines of the soft subgraph are gluons, and exactly one soft gluon enters  $H$ .

### 11.3 Factorization for DIS

To obtain factorization, we apply the steps listed in Sec. 11.1. Now that we have determined the leading and super-leading regions, it remains to apply Ward identities to sum over attachments of  $K$  gluons to the hard subgraph  $H$ . This will determine the operators defining parton densities.

As stated in Sec. 11.1, we now use Fig. 11.1(b) to refer to a generic term  $C_R \Gamma$  in the sum over regions and graphs, rather than just to specify a region. We also will generally impose a sum over graphs and regions. It is important to be conscious of the shifts in meaning of such a diagram.

It is convenient to combine the soft and collinear subgraphs into a single subgraph, and then to decompose all the external gluons of the hard subgraph  $H$  into  $K$  and  $G$  gluons. *The Ward identities are applied to gluonic external lines of the  $H$  bubble, which is treated as a sum over the possible graphs and equipped with subtractions for smaller regions.*

Now the hard factor in  $C(R)$  is defined to be expanded in powers of small momentum components, with retention of terms that contribute to the leading power or higher. Thus for a leading term, e.g., two  $G$  gluons plus any number of  $K$  gluons, the hard factor is simply taken with its external lines massless, on-shell at zero transverse momentum. As in our examples in previous chapters, this short-circuits integrals over  $k_j^-$  and  $k_{j,T}$ , so that the coordinate-space fields at the edges of the collinear-soft subgraph (and hence in the parton densities) are separated in the minus component of position, as in (7.40).

In situations where higher terms in the expansion of  $H$  in powers of  $k^-$  and  $k_T$  are used, we get extra factors of these momentum components. In the operator definitions of the collinear factors, these give derivatives with respect to the various  $x_T$  and  $x^+$  coordinates in the operators, with the derivatives taken at  $x_T = x^- = 0$ .

11.3.1 Abelian gluon

We start with the case of a model theory with an *abelian* gluon field, since its Ward identities are simple, as in Sec. 10.8.3.

We apply a Ward identity in turn to the attachment of each  $K$  gluon to the hard subgraph  $H$ , defined as the sum over graphs with a given number of external lines, with appropriate irreducibility properties, and with subtractions for smaller regions.

We get terms for attaching the  $K$  gluon to each of the external charged lines of the hard scattering. Just as with the Sudakov form factor, the Ward identities are unaffected by the presence of subtractions.

Case of all-gluon connection

When all the external lines of  $H$  are gluons, there are no external charged lines, so that summed over graphs, the attachment of a  $K$  gluon is zero:

$$\sum \text{Diagram} = 0 \tag{11.7}$$

The diagram shows a central oval labeled  $H$ . It has two wavy lines entering from the top, each labeled with momentum  $q$  and an arrow pointing towards the oval. It also has two wavy lines exiting from the top, each labeled with momentum  $q$  and an arrow pointing away from the oval. Below the oval, there are three vertical dashed lines representing gluon attachments, each starting from a solid triangle vertex pointing upwards towards the oval. The entire diagram is enclosed in a summation symbol  $\Sigma$ .

Here the solid triangle is the vertex for a  $K$  gluon, similarly to Fig. 10.6.

So we are left only with  $G$  gluons. For the leading power of  $Q$ , we keep the minimal number of gluons exchanged between the collinear and hard subgraphs. Since the case of one gluon gives exactly zero by charge-conjugation invariance, the minimum is two  $G$  gluons. Summing over attachments of  $K$  gluons to the hard subgraph gives zero. So the sum over all gluonic terms gives

$$\sum \text{Diagram} = \text{Diagram} + \text{power-suppressed} \tag{11.8}$$

The diagram on the left shows two ovals,  $H$  on top and  $C$  on bottom. Oval  $H$  has two wavy lines entering from the top (momentum  $q$ ) and two exiting (momentum  $q$ ). Oval  $C$  has two horizontal lines entering from the left (momentum  $P$ ) and two exiting to the right (momentum  $P$ ). They are connected by two vertical dashed lines. The diagram on the right is identical but the two vertical dashed lines are replaced by two vertical wavy lines, each with a cross on it. The entire diagram is enclosed in a summation symbol  $\Sigma$ .

In the main term on the r.h.s., the crosses denote what we now prove to be the vertices for the gluon density, as defined in (7.44).

Each cross starts out as a vertex  $G^{\mu_j \nu_j}$  for a  $G$  gluon; (11.6). The  $\mu_j = +$  case is zero, while the  $\mu_j = -$  term gives a power-suppressed contribution, by the boost argument in Sec. 5.8.8. This leaves the transverse components. The two  $G^{T\nu_j}$  factors are each  $1/k^+$  times the vertex for the gluon field strength tensor (Fig. 7.12). One factor of  $1/k^+$  gives the explicit  $1/\xi P^+$  in the definition of the gluon density (equation (7.44) and Fig. 7.9). The only difference with those formulae and Feynman rules is that there is no Wilson line in the gluon density in an abelian theory. The remaining  $1/k^+$  factor goes with the integral over  $k^+$  that joins the hard and collinear subgraphs, to give the  $d\xi/\xi$  factor in (8.81). According to the standard construction of a hard scattering, the external lines of the  $H$  subgraph are

set on-shell with zero transverse momentum; kinematically this is just as in the parton model. As in (7.44), we wrote the gluon density factor in the form  $\rho_{g,j'j}(\xi, S) f_g(\xi)$ , where  $\rho_{g,j'j}(\xi, S)$  is normalized to be a density matrix, i.e., it has trace unity.

As usual, renormalization is applied to the parton density. After we take the discontinuity of the uncut amplitude, we get the gluon term in the factorization theorem (8.81)

$$\int_{x^-}^{1+} \frac{d\xi}{\xi} C_g^{\mu\nu;j'j}(q, \xi P; \alpha_s, \mu) \rho_{g,j'j}(\xi, S; \mu) f_g(\xi; \mu). \tag{11.9}$$

Here we have inserted two (summed) transverse spin indices. For the common case of an unpolarized target, the gluon spin density matrix  $\rho_{g,j'j}$  is half the unit matrix. The normalization of the coefficient function  $C_g$  is exactly that of DIS on a transversely polarized on-shell gluonic target, with subtractions applied to cancel collinear divergences. As usual, the integral over gluon  $k^-$  and  $k_T$  is inside the standard definition of the gluon density.

*Quark-antiquark plus K gluons*

Since Faddeev-Popov ghosts are non-interacting in an abelian gauge theory in the gauges we use, the only other case that gives a leading contribution is where a quark and an antiquark line connect the collinear and hard subgraphs, together with any number of  $K$  gluons.

The Ward-identity argument works exactly as for collinear-to- $A$  gluons attaching to the hard scattering in the Sudakov form factor (Sec. 10.8). There the sum over  $K$  gluons gave a Wilson line at the collinear-to- $A$  quark entering the hard scattering.

For DIS the essential difference is that the hard scattering has both a quark and an antiquark external line, so that we get a Wilson line for each. The quark field  $\psi(0)$  in the parton density therefore becomes  $W(\infty, 0)\psi(0)$ , while the antiquark field has a Wilson line of the opposite charge:  $\bar{\psi}(w^-)W(\infty, w^-)^\dagger$ . The Wilson lines have zero transverse separation, so they can be combined to give a Wilson line between the two fields:  $[W(\infty, w^-)^\dagger W(\infty, 0) = W(w^-, 0)$ . The Wilson lines are in the light-like direction  $w_2$ , and the operators defining the quark density are exactly the ones in (7.40).

We must also apply the same leading-power approximations on the quark polarization as in the parton-model. Compared with the gauge-invariant parton model (Sec. 7.7), the new features are that we have arbitrarily higher-order corrections to the hard factor  $H$ , with subtractions as usual, and that the parton densities must be renormalized.

We write the overall result as

(11.10)

which gives the quark term in the factorization theorem.

### *Cancellation of rapidity divergences*

The key technical details of the full proof have involved a minor generalization of the methods we applied to the Sudakov form factor.

One notable difference is that the Wilson lines are light-like, which gives rapidity divergences graph-by-graph. But the divergences cancel in the final result. The easiest way of seeing this in general is to work in coordinate space and use the identity (7.39). Now the rapidity divergences are associated with on-shell Wilson-line denominators, and hence with a situation in which the Wilson line is infinitely long, i.e., when we integrate the vertices all the way to infinity. But (7.39) shows that the segment out to infinity cancels. As with our argument about the pinch singularities of  $T^{\mu\nu}$ , to use this argument in momentum space requires that we take a local average of the parton density over longitudinal momentum fraction. An example can be seen in our one-loop calculations in Sec. 9.4.3.

Because of the rapidity divergences at intermediate stages, it may be appropriate to use a non-light-like denominator  $k \cdot n$  until all the  $K$  gluons are extracted and converted to Wilson lines. After that one replaces  $n$  by a light-like vector  $w_2$ .

### *Overall view*

We now have completed the proof of factorization in the model theory. All the standard consequences follow, including the ability to implement perturbative calculations as explained in Ch. 9.

### **11.3.2 Non-abelian gluon**

In a non-abelian gauge theory like QCD, we have Slavnov-Taylor identities instead of simple Ward identities. They and their proof by direct diagrammatic methods are much more complicated than in the abelian case. In much of the original work on proving factorization the issues related to extracting  $K$  gluons from the hard scattering were glossed over.

Labastida and Sterman (1985) did give a diagrammatic proof of one critical result that one gets zero when all or all but one of the external lines of the hard scattering are  $K$  gluons. In Sec. 11.9, I will summarize an argument that generalizes to a non-abelian theory the Ward-identity methods for  $K$  gluons that were obtained for an abelian theory in Sec. 11.3.1.

But the proof only applies in the strictly collinear limit. Since individual contributing graphs are super-leading, this leaves open the possibility that there is a non-zero remainder of leading power. The remainder is power-suppressed with respect to the contributions of individual graphs, but not with respect to the final result. In fact, Collins and Rogers (2008) recently found by the simplest possible explicit calculation that the remainder is actually non-zero; the pure  $K$ -gluon terms contribute to the gluon density, unlike the case in an abelian gauge theory.

So more powerful methods are needed.

The ultimate result is standard factorization of the form (8.81), where each term is a coefficient convoluted with the matrix element of a gauge-invariant operator, and all the

relevant operators are the ones listed in (7.40) and (7.43) (generalized to include polarization effects). Essentially identical issues arose in the short-distance OPE for moments of DIS structure functions.

One possible approach to a proof is to generalize the diagrammatic arguments of Sec. 10.8.3, as in Labastida and Sterman (1985) and Sec. 11.9.

Instead we now use an argument using BRST invariance that has been used in the renormalization of gauge-invariant local operators; see Collins (1984, Sec. 12.6).

Without the use of gauge invariance, the structure of the leading regions, Fig. 11.1(b), leads to a factorization in which there is an infinite collection of operators; each different number of gluons gives a different pdf-like object, and for each extra gluon there is an extra longitudinal-momentum argument to be convoluted with the associated hard-scattering coefficient. If this were the whole story, the formalism would have little predictive power. But, in reality, terms differing by extra gluons have the same coefficient function, and the pdf-like objects all sum to a gauge-invariant pdf, with a single longitudinal-momentum variable  $\xi$ .

#### BRST restrictions on operators

A natural initial idea for the proof is that because QCD is color-gauge invariant, so are all the operators defining allowed parton densities. However, the actual QCD Lagrangian is not gauge invariant, but only BRST invariant (Sec. 3.1.3).

It is useful to generalize DIS to treat an off-shell Green function corresponding to the amplitude  $T^{\mu\nu}$ :

$$T_{\text{off-shell}}^{\mu\nu}(q) = \frac{1}{4\pi} \int d^4z e^{iq \cdot z} \langle 0 | T \text{ fields } j^\mu(z/2) j^\nu(-z/2) | 0 \rangle. \quad (11.11)$$

Here, “fields” denotes a product of two (or more) fields that are Fourier-transformed to be in a similar kinematic region to the target bra and ket,  $\langle P, S |$  and  $| P, S \rangle$  in (11.1). The derivation of leading regions works equally well for  $T_{\text{off-shell}}^{\mu\nu}(q)$  as it does for the normal on-shell tensor. Therefore, to leading power we obtain a sum (and convolution) over coefficients and pdf-like matrix elements:

$$T_{\text{off-shell}}^{\mu\nu}(q) = \sum_i C_i \otimes \langle 0 | T \text{ fields } \mathcal{O}_i | 0 \rangle + \text{p.s.c.} \quad (11.12)$$

We have a sum over possible operators  $\mathcal{O}_i$ , and a convolution with the longitudinal-momenta arguments of the operators. At this point in the argument there is the possibility that we have arbitrarily complicated multilocal operators, as pointed out above.

Now from BRST symmetry of the Lagrangian, there arises a conserved Noether current, and exactly as for an ordinary internal symmetry it follows that Green functions are BRST invariant, i.e.,

$$\delta_{\text{BRST}} \langle 0 | T \text{ any fields } | 0 \rangle = 0. \quad (11.13)$$

(See, e.g., Collins, 1984; Nakanishi and Ojima, 1990.) The BRST variations of individual fields are given in (3.6).

We apply (11.13) to (11.11). The electromagnetic currents are gauge invariant and hence BRST invariant. Therefore

$$\langle 0 | T (\delta_{\text{BRST}} \text{ fields}) j^\mu(z/2) j^\nu(-z/2) | 0 \rangle = 0. \tag{11.14}$$

Since the BRST variation adds a ghost field  $\eta$  (or removes an antighost field  $\bar{\eta}$ ), the interesting cases of this equation have one more antighost than ghost fields in “fields”.

Exactly the same formula must apply to the factorized form, up to possible power-suppressed terms:

$$\sum_i C_i(Q) \otimes \langle 0 | T (\delta_{\text{BRST}} \text{ fields}) \mathcal{O}_i | 0 \rangle = \text{p.s.c.} \tag{11.15}$$

We remove the power-suppressed corrections by defining the coefficient functions to be obtained from an expansion in powers of  $Q$  and  $\ln Q$ , and by restricting to the leading power of  $Q$ .<sup>2</sup>

Using (11.13), we get

$$\sum_i C_i \otimes \langle 0 | T \text{ fields } \delta_{\text{BRST}} \mathcal{O}_i | 0 \rangle = 0. \tag{11.16}$$

This is true no matter which set of fields is used, so the operators themselves are BRST invariant:

$$\delta_{\text{BRST}} \sum_i C_i \otimes \mathcal{O}_i = 0. \tag{11.17}$$

Factorization follows, generalized from (8.81) to apply to the off-shell amplitude  $T_{\text{off-shell}}^{\mu\nu}$ , and with the operators restricted to be BRST-invariant operators.

Up to here the derivation is identical to the one for the OPE, or for the renormalization of gauge-invariant operators.

Gauge-invariant operators are BRST invariant, so the important question is what other BRST-invariant operators exist. In the OPE, the operators  $\mathcal{O}_i$  are local, i.e., they are polynomials in elementary fields and their derivatives all at the same space-time point. In that case, we have a theorem (Joglekar and Lee, 1976; Joglekar, 1977a, b; Nakanishi and Ojima, 1990) that all the other possible operators are one of the following classes:

- A. operators that are BRST variations:  $A = \delta_{\text{BRST}} A_{\text{source}}$ ;
- B. operators that vanish by the equations of motion.

Operators in class B have vanishing matrix elements in on-shell states, but they contribute (Collins, 1984, p. 14) in time-ordered Green functions, because of the peculiarities of combining time-ordering of operators with derivatives of fields. The BRST invariance of operators in class A follows from the nilpotence of BRST transformations (up to terms vanishing by the equations of motion).

Operators in both of these classes vanish in on-shell matrix elements with physical states. This is trivial for operators vanishing by the equations of motion, and follows

<sup>2</sup> See Sect. 11.7 for variations on this expansion when quark masses may be non-negligible.

simply (Collins, 1984, p. 318) from BRST invariance of physical states for operators in class A.

A minor generalization of these results is that we also have vanishing contributions of operators of classes A and B in Green functions with gauge-invariant operators, as well as in matrix elements with physical scattering states. Equation-of-motion operators give delta functions in coordinate space in Green functions with other operators, and we can eliminate these by requiring the positions of the other operators to be away from the operators  $\mathcal{O}_i$ . The Green functions of BRST-variation operators with gauge-invariant (and indeed BRST-invariant) operators vanish by a simple application of (11.13).

Unfortunately, the published proofs that BRST-invariant operators are either gauge invariant or are in one of classes A or B apply as written to local operators. It is natural that the result also applies to the non-local operators we use in factorization. But, as far as I know, no proof has been given. For the purposes of the discussion, I will assume the result is true, and leave the proof (or refutation) to future research.

An example of a BRST-variation operator is

$$\begin{aligned} \delta_{\text{BRST}} [\bar{\eta}^\alpha(0, x^-, \mathbf{0}_T) A_\mu^\beta(0)] / \delta\lambda \\ = [\partial \cdot A^\alpha(0, x^-, \mathbf{0}_T) A_\mu^\beta(0)] + [\bar{\eta}^\alpha(0, x^-, \mathbf{0}_T) D_\mu^\beta \eta(0)]. \end{aligned} \quad (11.18)$$

The free Lorentz index  $\mu$  could be a  $-$  index (corresponding to the  $A^+$  component), or it could be a transverse index contracted with a transverse momentum somewhere.

I am not aware of an explicit calculation of the presence of such operators in calculations of factorization with off-shell Green functions. But there are calculations in the analogous case of the renormalization of local operators (Dixon and Taylor, 1974; Kluberg-Stern and Zuber, 1975), which showed the occurrence of non-gauge-invariant operators as counter-terms to local operators.

### *Gauge-invariant operators*

We now have the result that all the operators needed to apply factorization in physical matrix elements are gauge invariant. We call their matrix elements parton densities.

Obvious possibilities are the operators used to define gauge-invariant parton densities in (7.40) and (7.43). In each case we have a pair of basic partonic fields ( $\bar{\psi}$  and  $\psi$  or two field strength tensors) separated in the minus direction and connected by a Wilson line starting at one partonic operator and ending at the other. The representation of the gauge group in the Wilson line is the one appropriate to the partonic field. Each of the fields and the Wilson lines transforms covariantly under gauge transformations, e.g., (7.35), without derivatives, and it is then easy to deduce gauge invariance for the operators in the parton densities.

It is important to rule out other possibilities. Generalizations of this issue arise in dealing with power-law corrections where more complicated operators get used, and they also arise in treating transverse-momentum-dependent (TMD) parton densities, etc., where the Wilson lines may be non-light-like. Gauge invariance alone does not determine the path along which the gluon field is integrated in a Wilson line  $W(C)$ : the transformation law (7.35) involves only the endpoints of the path  $C$ , and is independent of which path is chosen

between the endpoints. As we have seen with the Sudakov form factor, the path should be one such that a factorization theorem can be derived.

For our case the requirements on the operators defining the parton densities are:

1. The operator is formed out of the elementary fields of the theory, and the elementary fields correspond to the lines entering the hard scattering.
2. Since the hard scattering is expanded in powers of  $k^-$  and  $k_T$ , for each parton line entering the hard-scattering subgraph, the parton density has the corresponding momentum components integrated over. In coordinate space the operators therefore have zero relative position in  $x^+$  and  $x_T$ . Thus the operators are localized on a line in the  $x^-$  direction.
3. By power-counting all but at most two of the elementary fields are  $A^+$ .

A simple way of dealing with this problem is to convert to light-cone gauge  $A^+ = 0$ . That eliminates all the extra gluons entering the hard scattering. The operators are now the same as in the elementary parton model without gauge links. Since the standard gauge links in the minus direction are unity in  $A^+ = 0$  gauge, one can insert the standard gauge links and recover the standard gauge-invariant links.

But given the known problems with  $A^+ = 0$  gauge, it would be nice to have a proof that does not rely on the gauge.

Since the Wilson line is restricted to a line in the  $x^-$  direction, the results of Sec. 7.5.2 show that the results now depend only on the endpoints of the path, at 0 and at  $(0, x^-, \mathbf{0}_T)$ . So we can choose the path just as we did when we first defined gauge-invariant parton densities, in Secs. 7.5.4 and 7.5.5.

We will see in Ch. 13 that the case of TMD densities shows a notable contrast, because for TMD densities the path in the Wilson line has segments at different transverse positions.

## 11.4 Renormalization of parton densities, DGLAP evolution

We will also need the DGLAP equations for the evolution of the parton densities:

$$\frac{d}{d \ln \mu} f_{j/H}(\xi; \mu) = \sum_{j'} \int \frac{dz}{z} 2P_{jj'}(z, g) f_{j'/H}(\xi/z; \mu), \quad (11.19)$$

As explained in Sec. 8.4, these equations are the RG equations for the parton densities, and the kernels can be computed from the renormalization coefficients; see (8.31)–(8.33).

Compared with that section, the main difference in the derivations for QCD is the same as for factorization in QCD compared with factorization in non-gauge theories. This is that there can be arbitrarily many  $K$  gluons connecting the collinear subgraph to the hard subgraph. For the case of renormalization, a hard subgraph is a subgraph whose loop integration gives a UV divergence. The possible operators used in renormalization are organized into the same classes: the standard gauge-invariant operators, BRST variations, and operators that vanish by the equations of motion. For the same reasons as with the local operators used in the OPE (Collins, 1984, p. 318), the renormalization matrix has a

triangular form:

$$\begin{pmatrix} \mathcal{O} \\ \mathcal{A} \\ \mathcal{B} \end{pmatrix} = \begin{pmatrix} Z_{\mathcal{O}\mathcal{O}} & Z_{\mathcal{O}A} & Z_{\mathcal{O}B} \\ 0 & Z_{AA} & Z_{AB} \\ 0 & 0 & Z_{BB} \end{pmatrix} \begin{pmatrix} \mathcal{O}_{(0)} \\ \mathcal{A}_{(0)} \\ \mathcal{B}_{(0)} \end{pmatrix}. \quad (11.20)$$

Here  $\mathcal{O}$  denotes the collection of gauge-invariant operators for the parton densities, while  $A$  and  $B$  denote the operators of classes A and B; see p. 409. The symbols  $\mathcal{O}_{(0)}$  etc. with a subscript (0) denote the bare operators, and the unadorned symbols denote renormalized operators.

In physical matrix elements, only the operators  $\mathcal{O}$  are non-zero, so that the normal DGLAP kernels can be computed from the  $Z_{\mathcal{O}\mathcal{O}}$  factors alone. In physical calculations, we can therefore replace (11.20) by  $\mathcal{O} = Z_{\mathcal{O}\mathcal{O}}\mathcal{O}_{(0)}$ .

At one-loop order, all the necessary calculations can be performed (Sec. 9.4) with on-shell matrix elements in quark and gluon states; hence there is no need to treat the extra operators  $A$  and  $B$ . But a correct treatment of renormalization beyond one-loop order needs to take account of the presence of other operators in renormalization of the operators in off-shell Green functions. Cf. Hamberg and van Neerven (1992) and Collins and Scalise (1994).

## 11.5 DIS with weak interactions

So far in this chapter, we have worked with DIS with photon exchange, so that there are electromagnetic currents in the definition of  $W^{\mu\nu}$ . All the same methods and ideas work identically for other processes, with  $Z$  and  $W$  boson exchange. See Sec. 7.1 for an account of the structure functions and the application of the parton model, which corresponds to the LO QCD approximation. Naturally, the parton model is supplemented by an application of DGLAP evolution, and by the use of higher-order corrections to the hard scattering.

## 11.6 Polarized DIS, especially transverse polarization

So far, this chapter's treatment has (mostly implicitly) allowed for general polarization states for the target and the partons, so that factorization was derived in the form (8.81), with a helicity density matrix for the parton initiating the hard scattering. In a non-gauge theory, we projected this onto factorization for individual structure functions in (8.83). There  $F_1$  and  $F_2$  use unpolarized parton densities  $f_j(\xi)$ ,  $g_1$  uses the helicity densities  $\Delta f_j(\xi)$ , and  $g_2$  is zero at the leading-power level (so that the transversity densities  $\delta_T f_j(\xi)$  do not appear).

The derivation of these results is entirely unchanged in QCD. First, there is the classification of parton densities into unpolarized densities, helicity densities, and transversity densities (with a generalization for spin-1 gluons and for targets of spin other than  $\frac{1}{2}$ ). The derivation of the classification in Secs. 6.4 and 6.5 used parity invariance and angular-momentum conservation about the  $z$  axis. This derivation is affected neither by inserting Wilson lines in the minus direction in the operator definitions of the parton densities nor

by renormalization. As for the hard scattering, the derivation of the form of polarization dependence is unchanged from that in a non-gauge theory in Sec. 8.10. Notably there is no change in the proof in Sec. 8.10.5 that at leading power there is no contribution from transverse spin.

## 11.7 Quark masses

We obtained factorization by an expansion to the leading power of an appropriate large scale  $Q$  (with logarithms of  $Q$  being allowed for). This implies setting masses to zero in the hard scattering, thereby entailing the assumption that masses are all much less than  $Q$ . But in reality this is not always the case. Relevant experiments in DIS and other processes currently range from  $Q$  below 2 GeV to many hundreds of GeV, which more than spans the masses of the charm, bottom, and top quarks.

Evidently we must generalize our formulation of factorization to correctly treat heavy quarks. I will not give a complete treatment, but just summarize the results. The essential insights are in the decoupling theorem of Appelquist and Carazzone (1975) and in the work of Witten (1976) on the contributions of heavy quarks to DIS in the framework of the OPE. We saw the underlying ideas in Secs. 3.9–3.11.

The basic observation is that if the mass of a particular field in a QFT is much bigger than the momentum scale of a process, then we can drop that field from consideration with errors suppressed by a power of the heavy quark relative to the process's scale. Because of the need for renormalization, the decoupling theorem modifies this by showing that the values of renormalized parameters may need to be adjusted after dropping the heavy quarks.

Complications arise because in a reaction with a hard scale, like DIS, there are two momentum scales:  $Q$  and  $\Lambda$ . For example, a mass  $m_q$  may be small relative to  $Q$ , but not relative to  $\Lambda$ . In that case, we might want to neglect  $m_q$  with respect to  $Q$ , but also we might want to perform the opposite operation, decoupling of the quark, with respect to low-energy phenomena. Moreover, the simplest applications have errors of the order of ratios like  $m_q/Q$ , whereas we would like factorization to be valid up to power corrections in the smallest ratio  $\Lambda/Q$  uniformly as we vary the relative sizes of  $Q$  and the heavy quark masses.

We distinguish four cases with corresponding approximation methods:

- $m_q \gg Q$ . Then we simply decouple the heavy quark.
- $m_q \sim Q$ . Then we must keep the heavy quark's mass unapproximated in the hard scattering. We can apply the decoupling theorem to the parton densities, in such a way that the sum over quark flavors in the factorization theorem is restricted to the lighter quarks.
- $Q \gg m_q \gg \Lambda$ . Then we can neglect  $m_q$  in the hard scattering, and we treat the quark like a light quark. But we apply a modified decoupling theorem to compute the evolved heavy quark distribution in terms of the light-parton distributions.
- $m_q \lesssim \Lambda$ . The quark is a light parton, so that the methods we have derived so far are valid.

To get the best accuracy uniformly in the relative sizes of  $Q$  and the heavy quark masses, a combination of the basic approximation methods is needed, with possibly different methods being applied to different quarks.

The solution is not unique, and a variety of methods can be found in the literature, as reviewed in Thorne and Tung (2008), although not all are equally adequate. However, the variety is much less if one insists that the methods apply to all cases rather than just the limiting cases  $m_q \ll Q$  and  $m_q \gg Q$ , and if one insists that there must be a definite gauge-invariant operator definition of every parton density. (An operator definition ensures that one actually knows the meaning of the concept of a parton density.)

I adopt the scheme of Collins, Wilczek, and Zee (1978) (CWZ), as extended to parton densities by Collins and Tung (1986); see Sec. 3.10. This involves a sequence of renormalization subschemes, parameterized by the number of “active quark flavors”  $n_{\text{act}}$ . Counterterms for graphs containing only the lightest  $n_{\text{act}}$  flavors are renormalized by the  $\overline{\text{MS}}$  method, and the heavier quarks by zero-momentum subtractions, which continue to preserve gauge invariance automatically. Manifest decoupling occurs when the masses of inactive quarks are much larger than the scale of the process; graphs containing the inactive quarks are then power-suppressed, and can be simply dropped. Matching calculations between the subschemes have been performed (Chetyrkin, Kniehl, and Steinhauser, 1997, 1998; Aivazis *et al.*, 1994).

In a particular subscheme, the evolution equations, both the RGE for the QCD parameters and the DGLAP equations for the parton densities, are exactly those in the  $\overline{\text{MS}}$  scheme with  $n_{\text{act}}$  quarks. One then talks of a 3-flavor scheme, a 4-flavor scheme, etc.

A straightforward generalization of the factorization property is set up by choosing the active flavors to be those for which  $m_q \lesssim Q$ . The sum over flavors in (8.81) etc. is then only over active flavors. Masses of heavy quarks, and especially of inactive quarks, are not neglected in the hard scattering, unless  $m_q \ll Q$ . This method was first proposed by Aivazis *et al.* (1994) (ACOT). It has the following consequences:

- In the hard scattering, inactive quarks can appear as internal lines.
- Parton densities for inactive quarks are suppressed by a power of  $\Lambda/m_q$  and are generally dropped. But this is not required.
- When the mass of some heavy quark  $m_q$  is much larger than  $Q$ , there is a power-suppression of graphs containing this quark. Such graphs may be dropped, with an error suppressed by a power of  $Q/m_q$ .
- But when the mass is comparable with  $Q$ , there is no power-suppression.
- When the mass of a quark is much less than  $Q$ , its mass can be neglected in the hard scattering; such a quark is always an active quark.

When the mass of some heavy quark (notably charm or bottom) is comparable to  $Q$ , that quark may be legitimately treated either as active or as inactive, by a change of subscheme. Equivalent accuracy is obtained provided that the mass of that quark is retained in the hard scattering, at least when the quark is internal and the hard scattering is initiated by a lighter parton (e.g., a gluon).

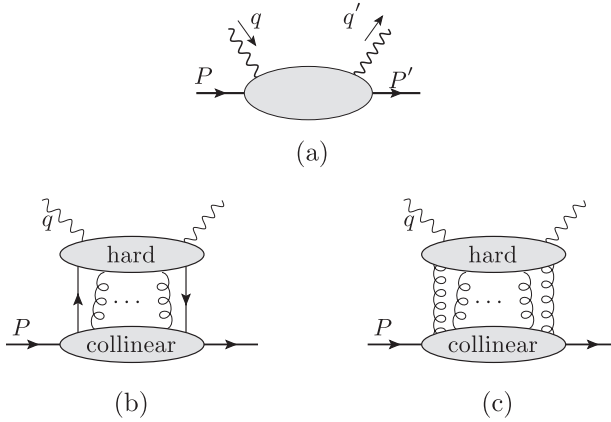


Fig. 11.5. (a) Uncut amplitude for DVCS or DIS. (b) and (c) Leading regions.

However, it is generally best if the mass of the parton initiating the hard scattering is replaced by zero. Also some kinematic modifications to the hard scattering improve its match to the physics. Tung, Kretzer, and Schmidt (2002) have provided a suitable implementation, which they call the ACOT( $\chi$ ) scheme.

### 11.8 DVCS and DDVCS

One quite simple extension of factorization for DIS is to a quantity like the DIS structure tensor  $W^{\mu\nu}$ , but where the two target states have different momenta  $P$  and  $P'$  and where the current operators are time ordered:

$$T^{\mu\nu}(q, P, P') = \frac{1}{4\pi} \int d^4z e^{iz \cdot (q+q')/2} \langle P' | T J^\mu(z/2) J^\nu(-z/2) | P \rangle. \quad (11.21)$$

Thus we have an uncut off-diagonal amplitude, Fig. 11.5(a), with incoming momentum  $q$  on the photon at  $J^\nu(-z/2)$ , and outgoing momentum  $q' = q + P - P'$  on the photon at  $J^\mu(z/2)$ . The process is  $\gamma^*(q) + P \rightarrow \gamma^*(q') + P'$ .

Realizable physical processes using this amplitude are deeply virtual Compton scattering (DVCS), and double deeply virtual Compton scattering (DDVCS):

- DVCS:  $e + P \rightarrow e + \gamma + P'$ ;
- DDVCS:  $e + P \rightarrow e + \mu^+ \mu^- + P'$ .

In both cases the incoming virtual photon in Fig. 11.5(a) is space-like and is exchanged with the same kind of lepton as in ordinary DIS. In DVCS the outgoing photon is real, while in DDVCS the outgoing photon is virtual and time-like, generating a lepton pair.

We obtain factorization by a minor generalization of the method used for the *uncut* amplitude (11.1) for DIS. For DDVCS, the regions have exactly the same form, and so do the leading regions.

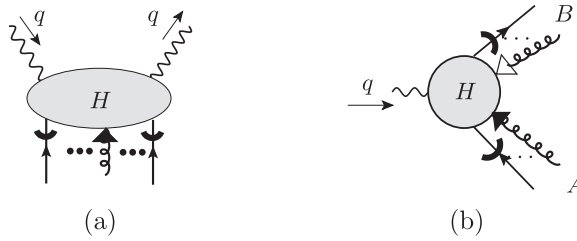


Fig. 11.6. Hard subgraph  $H$  with  $K$  gluons attached. The thick curved lines indicate where an external quark is set on-shell in  $H$ . The triangle indicates the application of a Grammer-Yennie  $K$  approximant, defined as in Sec. 10.4.2. Graph (a) is for DIS, with one collinear subgraph. Graph (b) is for  $e^+e^-$  annihilation in the simplest case of two collinear groups. Here the solid arrow denotes the approximant for collinear- $A$  gluons and the open arrow denotes the approximant for collinear- $B$  gluons.

But for DVCS, it is possible to have regions with a group collinear to the outgoing real photon, Fig. 5.16(a). After allowing for the usual Grammer-Yennie cancellation of  $K$  gluons, all these extra regions are power-suppressed, and the leading regions are the same as for DDVCS.

In both cases, the factorization theorem has the same form as for DIS except that the parton density is replaced by a generalized parton density (GPD) (6.90), whose definition differs from that for an ordinary parton density simply by being off-diagonal in the target state. Equation (6.90) was written for the case of super-renormalizable non-gauge theory, and for a quark. The structural modifications to treat renormalization, to insert a Wilson line, and to define a gluon density are the same as in ordinary pdfs. The DGLAP kernels have to be generalized, and include dependence on the longitudinal momentum transfer. See Diehl (2003) for a review.

### 11.9 Ward identities to convert $K$ gluons to Wilson line

This section gives a graphical proof of the conversion of  $K$  gluons from attachments to a particular kind of subgraph to couplings to a Wilson line. It generalizes to non-abelian gauge theories and to other processes the work done in Ch. 10 for the Sudakov form factor in an abelian gauge theory.

#### 11.9.1 Statement of general situation

In a gauge theory, we consider a subgraph for a particular momentum category to which Grammer-Yennie  $K$  gluons attach from a subgraph for another momentum category. One example is a hard scattering, where the  $K$  gluons come from collinear subgraph(s), Fig. 11.6. Another example is a collinear subgraph with soft  $K$  gluons attached, Fig. 11.7.

Each  $K$ -gluon attachment, notated by a triangle, represents an approximant of the form

$$H(k)_\mu g^{\mu\nu} A(k)_\nu \mapsto H(\hat{k})_\mu \frac{\hat{k}^\mu n_2^\nu}{k \cdot n_2} A(k)_\nu, \tag{11.22a}$$

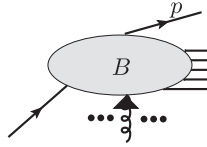


Fig. 11.7. Collinear subgraph  $B$  with  $K$  gluons attached. The subgraph is written for the amplitude for a quark to produce a jet of hadrons in which a hadron of momentum  $p$  is detected. The final state on the right consists of on-shell physical particles. The quark has come out of the hard scattering, as in  $e^+ + e^-$  annihilation to hadrons; see Ch. 12. Unlike the case of Fig. 11.6, the external left-hand quark line is off-shell and includes a full propagator.

where the approximated momentum is

$$\hat{k}^\mu = n_1^\mu \frac{k \cdot n_2}{n_1 \cdot n_2}. \tag{11.22b}$$

The vector,  $n_1$ , normally light-like, is the direction of the approximated momentum (e.g.,  $(1, 0, \mathbf{0}_T)$  in  $H$  in DIS). The vector  $n_2$  is either a conjugate light-like vector (e.g.,  $(0, 1, \mathbf{0}_T)$  in DIS) or is close to such a vector, to regulate rapidity divergences.

### 11.9.2 Proof for $H$ in DIS

In this section, we treat the hard-scattering subgraph  $H$  for DIS, Fig. 11.6(a). Subtractions have been applied, as in Sec. 10.8, to remove contributions from smaller regions. We assume that the subtractions do not interfere with the Ward identities, as we saw in Sec. 10.8.

In that section the Ward identities were for an abelian theory, and used the basic diagrammatic elements listed in Sec. 10.8.3. Our task now is to generalize that argument to a non-abelian theory.

Consider first one  $K$  gluon. It has a factor of  $\hat{k}$  contracted into some Green function. If this were a complete Green function, then, as explained in Sterman (1993, p. 351), we obtain a ghost attachment to each gauge-variant external line of the Green function:

$$\text{Diagram} = \sum \text{Diagram 1} + \sum \text{Diagram 2} \tag{11.23}$$

On the l.h.s., a full propagator is amputated for the  $K$  gluon. On the r.h.s. the sums are over the gauge-variant external fields of the Green function, and the special vertices with a thick diagonal line are the BRST variations of the external fields. In the first term, the (amputated) gluon directly attaches to the BRST variation of the external field, exactly as in an abelian theory. The thin diagonal line denotes the remaining factor  $-in_2/(k \cdot n_2)$ , from (11.22a), together with a normalization factor  $-i$ . In the second term, the diagonal line replaces the incoming ghost line at a ghost-gluon vertex. The ghost line continues to

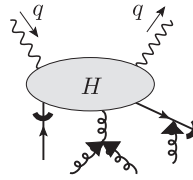


Fig. 11.8. Graphs such as these are *not* included in  $H$  because they are reducible in collinear lines.

the BRST variation of an external field. This Slavnov-Taylor identity applies in the form stated to ordinary Green functions, which are expectation values of time-ordered products of fields.

But in our case the Green functions have particular irreducibility properties. The graphs for  $H$  are irreducible in the collinear lines. Not only are the external collinear lines amputated, but any graphs in which collinear lines combine to a single line are omitted, as in Fig. 11.8.

To understand the consequences, we use the diagrammatic method of 't Hooft and Veltman (1972), which generalizes the formulation used in an abelian theory, in Sec. 10.8.3. This allows us to take account of missing items relative to the standard Slavnov-Taylor identity.

In Fig. 11.9 are shown some of the main graphical identities used in the proof in 't Hooft and Veltman (1972); this generalizes Fig. 10.12. We start by applying the line identities Fig. 11.9(a) and (b) to a  $K$  gluon. In an abelian theory, we completed the derivation of the Ward identities by applying vertex identities like Fig. 11.9(c).

But in a non-abelian theory, the ghost line is interacting, giving the second and fourth terms on the r.h.s. of Fig. 11.9(b). These require a recursive reapplication of the line identities, together with a further complication with ghost loops. After that we get a chain of cancellations at interaction vertices, from Fig. 11.9(c) and (d). With a regular Green function and a single  $K$  gluon, we get (11.23).

Now consider Fig. 11.6(a), with  $N$   $K$  gluons of incoming approximated momenta  $\hat{k}_1, \dots, \hat{k}_N$  attaching to  $H$ . We apply the diagrammatic proof of the Slavnov-Taylor identity to the first gluon. The standard chain of cancellations occurs except at vertices where the external lines from the collinear subgraph attach. Collinear irreducibility of  $H$  prevents certain terms from occurring. The missing terms are certain BRST-variation terms in a vertex identity like Fig. 11.9(c). Now each BRST-variation term is obtained from a line identity applied to a graph where the ghost field attaches at a vertex on the immediately neighboring line. The term is missing if and only if the graph is one prohibited by the irreducibility requirements.

The first case is where a term for the BRST variation of each quark line is missing. This gives an external line coupling for the gluon, one term for each quark (or antiquark) that is exactly of the Wilson-line form; this is no different than for an abelian theory. Application of the argument multiple times will give terms of the form of Fig. 11.10 with multiple external gluon attachments.

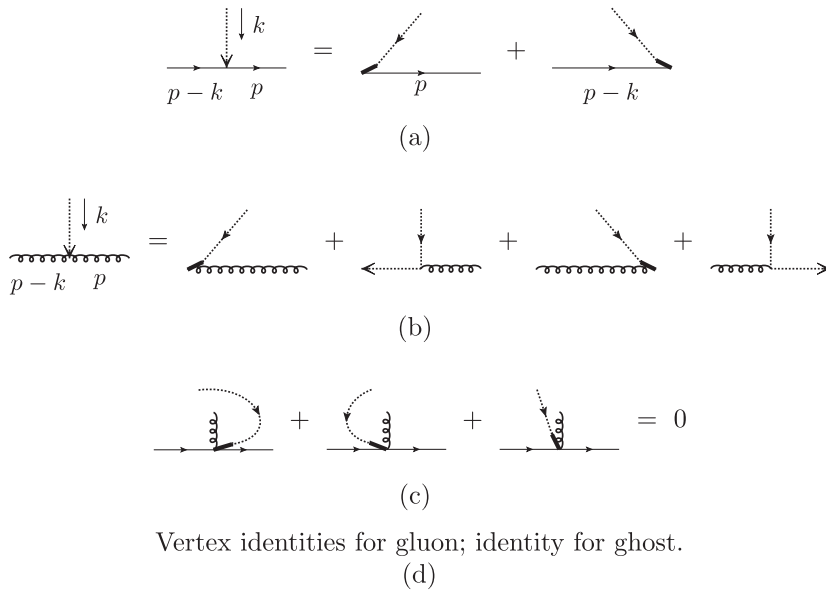


Fig. 11.9. Graphical elements of Ward identity in non-abelian gauge theory. (a) Line identity for quark. On the l.h.s., the arrow on the ghost line of momentum  $k$  represents a factor of  $k$  contracted into a *gluon* vertex for the quark. On the r.h.s., the thick diagonal lines represent a vertex for the BRST transformation on the field at the end of the quark line (multiplied by a factor  $-i$ ). (b) Line identity for gluon. (c) Vertex identity for quark-gluon vertex. There is a term for the color transformation of each field at the vertex. (d) The remaining identities can be found from 't Hooft and Veltman (1972).

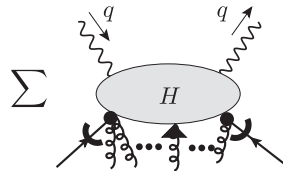


Fig. 11.10. Result after applying Ward identities to some  $K$  gluons. The little black blobs denote a vertex whose form we do not need to specify.

But in a non-abelian theory, there are additional terms. First, we observe that in the recursive application of the line identity of Fig. 11.9(b) there can be a term where one of the gluons is another  $K$  gluon with momentum  $p$ . Then the corresponding term on the right of the identity is zero. This is because the l.h.s. Fig. 11.9(b), with approximated momenta, is proportional to

$$[(\hat{p} - \hat{k})^\mu (\hat{p} - \hat{k})^\nu - g^{\mu\nu} (\hat{p} - \hat{k})^2] - [\hat{p}^\mu \hat{p}^\nu - g^{\mu\nu} \hat{p}^2]. \tag{11.24}$$

So contraction with  $\hat{p}_\nu$  makes its term zero, and no special term arises here.

Next, for a normal Slavnov-Taylor identity we have cancellations by vertex identities like Fig. 11.9(c). For a collinear-irreducible hard subgraph, there are some missing terms.

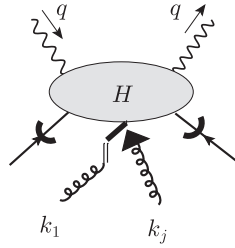


Fig. 11.11. Missing term in elementary Ward identity for connection to another *K* gluon. We will call these commutator terms between two *K* gluons.

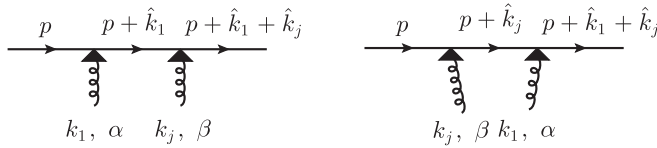


Fig. 11.12. Two ways of attaching neighboring *K* gluons to a quark line.  $\alpha$  and  $\beta$  are color indices.

Beyond the external-line terms already noted, we have missing terms involving other *K* gluons. The generic case is typified by Fig. 11.9(c), whenever the ghost line directly corresponds to the  $k_1$  gluon without any interactions and the explicit gluon is a *K* gluon. The missing term is the third term in Fig. 11.9(c); it would arise from attaching the two *K* gluons together before they enter the *H* subgraph, which is one of the disallowed situations. A possible notation for the general case is Fig. 11.11.

To see the meaning of the term, consider the example in Fig. 11.12. The first gluon, to which we are applying Ward identities, is  $k_1$  and it attaches to a quark line. Next to it is another *K* gluon, of momentum  $k_j$ . The sum of the two (approximated) graphs is

$$\frac{i}{\not{p} + \hat{k}_1 + \hat{k}_j} \left[ \frac{-igt_\beta \hat{k}_j}{k_j \cdot n_2} \frac{i}{\not{p} + \hat{k}_1} \frac{-igt_\alpha \hat{k}_1}{k_1 \cdot n_2} + \frac{-igt_\alpha \hat{k}_1}{k_1 \cdot n_2} \frac{i}{\not{p} + \hat{k}_j} \frac{-igt_\beta \hat{k}_j}{k_j \cdot n_2} \right] \frac{i}{\not{p}}. \quad (11.25)$$

We apply the basic line identity Fig. 11.9 to gluon  $k_1$ , by writing  $\hat{k}_1 = \not{p} + \hat{k}_1 - \not{p}$  in the first term and  $\hat{k}_1 = (\not{p} + \hat{k}_1 + \hat{k}_j) - (\not{p} + \hat{k}_j)$  in the second. We retain only the terms where the quark propagator between the gluons is canceled; this corresponds to a case of Fig. 11.11, and gives

$$\frac{i}{\not{p} + \hat{k}_1 + \hat{k}_j} \frac{ig^2 [t_\alpha, t_\beta] \hat{k}_j}{k_1 \cdot n_2 k_j \cdot n_2} \frac{i}{\not{p}} = \frac{i}{\not{p} + \hat{k}_1 + \hat{k}_j} (-igt_\gamma \hat{k}_j) \frac{i}{\not{p}} \frac{-igf_{\alpha\beta\gamma}}{k_1 \cdot n_2 k_j \cdot n_2}. \quad (11.26)$$

This term is of the form of a vertex for one gluon times some factor associated with the gluon pair. This factor is the composite vertex in Fig. 11.11, and is the same in all these situations.

We would like to apply a Ward identity to this new object. To do this we observe that the approximated momenta are parallel, and that  $k_j \cdot n_2 = \hat{k}_j \cdot n_2$ . Thus we can scale the numerator and denominator at the vertex so that the gluon-quark interaction is contracted

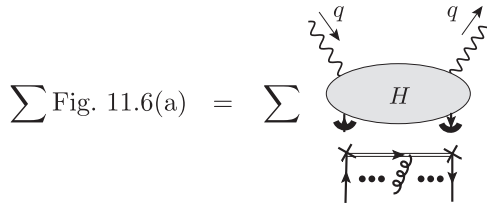


Fig. 11.13. After a sum over graphs in Fig. 11.6(a), the  $K$  gluons attach to a Wilson line appropriate for a gauge-invariant parton density.

with  $\hat{k}_1 + \hat{k}_j$  instead of  $\hat{k}_j$ , to obtain

$$\frac{i}{\not{p} + \hat{k}_1 + \hat{k}_j} \frac{-igt_\gamma(\hat{k}_1 + \hat{k}_j)}{(k_1 + k_j) \cdot n_2} \frac{i}{\not{p}} \frac{-igf_{\alpha\beta\gamma}}{k_1 \cdot n_2}. \tag{11.27}$$

We now have exactly a factor for an effective  $K$  gluon of momentum  $k_1 + k_j$  times some other factor, and the new  $H$  factor has one  $K$  gluon less than before. So we keep reapplying the basic Ward-identity argument until all the  $K$  gluons have been extracted from  $H$ . At each intermediate stage we have a result of the form of Fig. 11.10. At the final stage we just have some external line factors, multiplying a version of  $H$  with no extra gluons at all.

However, we just know that the external-line factors are composed of many Wilson-line denominators, of a factor  $g$  for each gluon, and a product of  $SU(3)$  structure constants. But it could just be a complicated mess, not the desired Wilson line. What we do know is that the external-line factors depend only on the color of the external lines; they do not depend on the other details of  $H$ . So the same argument applies when we replace  $H$  by a Wilson line in direction  $n_2$ , and it gives the same external-line factors. Therefore the external-line factors are exactly a Wilson line, i.e., we get Fig. 11.13, our final result.

### 11.9.3 Unapproximated gluon momenta

Notice that because the approximated momenta of the  $K$  gluons,  $\hat{k}_j$ , are all parallel, the transition from (11.26) to (11.27) is exact, as are the Slavnov-Taylor-Ward identities. So the conversion to a Wilson-line form is exact, with no left-over terms.

If instead we had chosen to leave the  $k_j$  momenta unapproximated in  $H$ , as in the original Grammer-Yennie paper, then we would have extra remainder terms. These would be power-suppressed in the collinear limit for all the  $K$  gluons. But when we integrate over all momenta, as in defining a parton density, then the remainder terms would be important outside the collinear region and would have to be taken into account. This would evidently be rather complicated if we tried to do it in general.

However, the use of unapproximated momenta can help at intermediate stages when dealing with super-leading contributions. In that case we would replace the vertices in (11.26) and (11.27) by

$$(-igt_\gamma k_j) \frac{-igf_{\alpha\beta\gamma}}{k_1 \cdot n_2 k_j \cdot n_2}, \tag{11.28}$$

and

$$\frac{-igt_\gamma(\not{k}_1 + \not{k}_j)}{(k_1 + k_j) \cdot n_2} \frac{-igf_{\alpha\beta\gamma}}{k_1 \cdot n_2}. \quad (11.29)$$

The difference is the part of (11.28) which is not treated recursively as a  $K$  gluon. It has a rather symmetrical form:

$$(-igt_\gamma\gamma_\mu) \frac{-igf_{\alpha\beta\gamma}}{(k_1 + k_j) \cdot n_2} \left[ \frac{k_j^\mu}{k_j \cdot n_2} - \frac{k_1^\mu}{k_1 \cdot n_2} \right]. \quad (11.30)$$

It is easily checked that, in the collinear limit, this is suppressed relative to the main effective  $K$  term (11.29) by a power of small components of  $k_1$  and  $k_j$  relative to large components. Expression (11.30) is written as a factor of a quark-gluon vertex times a factor. It can be checked that this factor is just derived from the commutator term in Fig. 11.11, so it applies in all situations, not just to the coupling to a quark, but to a gluon or a ghost.

#### 11.9.4 Including the case of all-gluon connections to $H$

Our proof of Fig. 11.13 applied directly to the case that the hard scattering is initiated by a quark and antiquark together with any number of  $K$  gluons.

The same principles apply when there are two  $G$  gluons plus any number of  $K$  gluons. But we also have to deal with the cases with super-leading contributions graph-by-graph. These are where (a) all the external lines of  $H$  are  $K$  gluons, and (b) one of the external lines is a  $G$  gluons and the rest  $K$  gluons.

When all the external lines are all  $K$  gluons, we start by applying our argument as it stands. Since there are no non- $K$  gluons, we get exactly zero. Thus the strongest super-leading term vanishes.

But there can be a leading remainder. In general, such a remainder is to be obtained by differentiating the hard scattering with respect to the small components of the collinear momenta, e.g.,  $k_{jT}$ . This would be complicated to deal with.

We rescue the situation by starting by applying the Ward-identity argument with unapproximated momenta. We start accumulating remainder terms (11.30) from the commutators. These we treat as generalizations to the  $G$ -gluon definition. Once we have two of them, we have a suppression from the  $Q^2$  super-leading power back to an ordinary leading power. At that point, the necessary suppression is exhibited in external factors, as in (11.30). From that point on, we can restore the approximations for the  $k_j$ s in the hard scattering, and drop any further accumulation of remainder terms.

We apply the same argument when there is one  $G$  gluon.

The end product of the argument is a hard scattering with either one or two external gluons containing factors appropriate for generalized  $G$  gluons. With one  $G$  gluon the hard scattering after application of the Ward-identity argument has a single external gluon; it therefore vanishes by color invariance. So we are left with two.

Application of the same argument to a product of two gluon field strength tensors joined by a Wilson line gives the same external factors. So the result should agree with the Feynman rules for an ordinary gluon density. A more explicit argument would be useful.

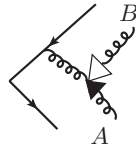


Fig. 11.14. Example of graph for a hard scattering that is one-particle reducible. But it is irreducible separately in the collinear group  $A$  of the lower two external lines and in the collinear group  $B$  of the upper two external lines. All external lines are amputated.

### 11.9.5 Generalizations

The proof in Sec. 11.9.2 generalizes in a relatively elementary way. We will deal with the modifications as needed. This notably concerns the soft-to-collinear case, which has some interesting differences, and which we will deal with in Sec. 12.8.3.

Relatively elementary generalizations concern different kinds of hard subgraph, and we summarize them here.

Trivial generalizations concern changing the nature or kinematics of the currents in Fig. 11.6. As long as they are gauge invariant (or even just BRST invariant), no change in the derivation is needed. Similarly, when we go to a collinear amplitude, we will generally have some on-shell hadrons in the initial or final state. As long as no irreducibility requirements are imposed, these give no contribution to the Ward identities.

The most important generalization is to hard scatterings where there are multiple collinear groups. The Sudakov form factor treated in Ch. 10 gives one example. The Drell-Yan process is another. The first case we will treat in QCD will be hadronic cross sections in  $e^+e^-$  annihilation, in Ch. 12.

We now discuss the simplest case of its hard-scattering amplitude as shown in Fig. 11.6(b). There is one (gauge-invariant) electromagnetic current, and two collinear groups,  $A$  and  $B$ . In the particular case shown, the partonic lines (always on-shell) are a quark and an antiquark, and any number of collinear  $K$  gluons.

The irreducibility requirements on  $H$  are now that it is irreducible in each group  $A$  and  $B$  separately; otherwise there would be an internal line of  $H$  forced to be collinear. But there is no restriction on combining lines from different collinear groups. An example is in Fig. 11.14.

For Fig. 11.6(b), we will use  $K$  gluons defined with the same collinear approximants that we defined in Sec. 10.4.2 for the Sudakov form factor. These have light-like auxiliary vectors  $w_1$  and  $w_2$ . The external quark and antiquark lines are defined so that they are on-shell with appropriate Dirac wave functions.

We start by applying Ward identities to a first  $K$  gluon from group  $A$ . As in DIS, the restriction to graphs irreducible in the  $A$  lines implies we obtain terms associated with the other collinear- $A$  lines. Repeated application of the Ward-identity argument converts these gluons into couplings to a Wilson line. This gives the middle graph in Fig. 11.15.

Some of the would-be cancellations involve moving the  $K$  gluons so as to uncover a graph irreducible in the  $B$  group. This is the same as for the Sudakov form factor in Sec. 10.8.6 with the one change that we can also implicate graphs involving pairs of  $K$

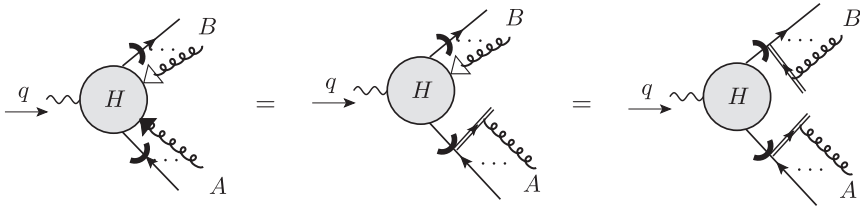


Fig. 11.15. Result of applying Ward identities to the  $K$  gluons of the  $A$  group, and then to the  $K$  gluons of the  $B$  group. The  $A$  gluons couple to a Wilson line in direction  $n_B$ , i.e., with rapidity  $-\infty$ . The  $B$  gluons couple to a Wilson line in direction  $n_A$ , i.e., with rapidity  $+\infty$ .

gluons from the  $B$  side as well as a  $K$  gluon and a quark. A typical non-canceling term of this kind is Fig. 10.20(c). But all of these terms are actually zero, because they involve a light-like collinear- $B$  momentum from a  $K$  gluon contracted into a non-singular subgraph with momenta all in the  $B$  direction.

In the case that we use massive external quarks, the cancellation is good to order  $m^2/Q^2$ , because the quark momentum differs by this much from being light-like. This is good enough to leading power.

So there are no extra terms, and the  $K$  gluons convert to a Wilson line.

Exactly the same argument applies for the  $B$  group, finally giving Fig. 11.15. This is the same result as with the Sudakov form factor, generalized to a non-abelian theory.

Most importantly, the same argument applies with minor changes when there are multiple collinear groups, and it also applies when some of the groups consist of all gluons (up to one  $G$  gluon). Each group  $\alpha$  has its direction defined by a light-like vector  $w_\alpha$ , together with a conjugate light-like vector  $\tilde{w}_\alpha$ . We can define

$$\tilde{w}_\alpha^\mu = \frac{q^\mu}{w_\alpha \cdot q} - \frac{w_\alpha^\mu q^2}{2(w_\alpha \cdot q)^2}. \tag{11.31}$$

This is a future-pointing light-like vector with its spatial component reversed compared to  $w_\alpha$ . It is also arranged so that  $w_\alpha \cdot \tilde{w}_\alpha = 1$ , which means that contracting a vector  $v$  onto  $\tilde{w}_\alpha$  and  $w_\alpha$  can be regarded as giving light-front plus and minus coordinates appropriate for the collinear group (i.e.,  $v^+ = v \cdot \tilde{w}_\alpha$  and  $v^- = v \cdot w_\alpha$ ).

The approximant for a  $K$  gluon of group  $\alpha$  to couple to the hard subgraph is a case of (11.22):

$$H(k_{\alpha i})^\mu C_\alpha(k)_\mu = H(\hat{k}_{\alpha i})^\mu \frac{\hat{k}_{\alpha i, \mu} \tilde{w}_\alpha^v}{k_{\alpha i} \cdot \tilde{w}_\alpha} C_\alpha(k)_v, \tag{11.32a}$$

where

$$\hat{k}_{\alpha i}^\mu = \frac{w_\alpha^\mu k_{\alpha i} \cdot \tilde{w}_\alpha}{w_\alpha \cdot \tilde{w}_\alpha}. \tag{11.32b}$$

The end result is that we have a hard scattering with one external on-shell line for each collinear group, and that we have a non-local vertex for each collinear group to attach to.

The non-local vertex is a natural generalization of what we have already seen in particular cases: a partonic field times a Wilson line that now goes out to infinity.

### Exercises

- 11.1** (No stars to (\*\*\*)) Examine the proofs for further weaknesses, and correct them as best you can.
- 11.2** ((\* to (\*\*\*)) One part of our proof of factorization for DIS in QCD relied on BRST properties of operators used in defining parton densities. The published proofs of these BRST properties (Joglekar and Lee, 1976; Joglekar, 1977a, b; Nakanishi and Ojima, 1990) are restricted to *local* operators, i.e., those that are products of field operators at a single space-time point. Work through these proofs (and check them!). Do they apply more generally, to the non-local operators defining parton densities? Why? If not, construct (and publish) a correct proof.
- 11.3** (\*\*\*) Characterize the non-gauge-invariant operators that appear in DIS on an off-shell target, with a particular emphasis on finding those that include Faddeev-Popov ghost fields.

It might be worth starting with some sample Feynman-graph calculations to get some inspiration. You should try to verify that the operators are BRST invariant.

From Fig. 11.4, you can see that the lowest-order graphs for ghost-induced hard scattering in ordinary DIS have two loops, which will probably make calculational examples hard. So you might also want to investigate a generalization of DIS in which the electromagnetic current operators are replaced by a gauge-invariant gluon operator, e.g.,  $G_{\mu\nu}^2$ . You could also examine renormalization of the gluon density, since the counterterms generally use the operator matrix elements as those used for parton densities in factorization.

- 11.4** (\*\*\*) Particularly if you have a sufficiently good theory of the necessary operators, it would be useful to examine renormalization, especially, one order beyond the lowest order where Faddeev-Popov ghosts appear. Examine the implications for calculations of the DGLAP kernel etc., and compare with Hamberg and van Neerven (1992) and Collins and Scalise (1994).